

The Adiabatic Energy Change of Plasma Electrons and the Frame Dependence of the Cross-Shock Potential at Collisionless Magnetosonic Shock Waves

C. C. GOODRICH

Department of Physics and Astronomy, University of Maryland, College Park

J. D. SCUDDER

Laboratory for Extraterrestrial Physics, NASA Goddard Space Flight Center, Greenbelt, Maryland

In collisionless magnetosonic shock waves, ions are commonly thought to be decelerated by a dc electrostatic cross-shock electric field along the shock normal \hat{n} . In a frame where ions are normally incident to the shock the change in the potential energy $[q\phi^N]$ in the quasi-perpendicular geometry is of the order of the change of the energy of normal ion flow: $[q\phi^N] \approx [\frac{1}{2}m_i(V_i^N \cdot \hat{n})^2]$, which is approximately 200–500 eV at the earth's bow shock. We show that the electron energy gain, typically $\frac{1}{10}$ this number, is consistent with such a large potential jump in this geometry. Key facts are the different paths taken by electrons and ions through the shock wave and the frame dependence of the potential jump in this geometry. In the normal incidence frame, electrons lose energy by doing work against the solar wind motional electric field \mathbf{E}_M^N , which partially offsets the energy gain from the cross-shock electrostatic potential energy $[e\phi_*^N]$. In the de Hoffman–Teller frame the motional electric field vanishes; the electrons gain the full electrostatic potential energy jump $e[\phi_*^{\text{HT}}]$ of that frame, which is not, however, equal to the electrostatic potential energy jump $e[\phi_*^N]$ in the normal incidence frame. We estimate the ratio of these potential jumps to be $[\phi_*^{\text{HT}}]/[\phi_*^N] \approx \gamma/(\gamma - 1)[kT_e]\{[-\frac{1}{2}m_i(V_i^N \cdot \hat{n})^2]\}^{-1}$, where γ is the effective polytropic index for electrons. By observation this ratio is $\sim \frac{1}{10}$ at the earth's bow shock. When viewed in the de Hoffman–Teller frame, corresponding changes in the ion kinematics occur. Since the $e[\phi_*^{\text{HT}}]$ is an order of magnitude smaller than the ion energy, the ions are not significantly affected by the electrostatic force. They are instead primarily retarded in this frame by the magnetic force. Since this latter force is proportional to the component of \mathbf{B} out of the coplanarity plane, infinitesimally thin shock models may not be realistic for the study of the ion and electron dynamics in the de Hoffman–Teller frame.

1. INTRODUCTION

It is generally recognized that an electrostatic field must exist across collisionless magnetosonic shock waves. This field is instrumental in decelerating the incoming plasma from a super- to a sub-fast-mode speed. The magnitude of the jump in the shock electrical potential for a path along the shock normal $[\phi]$ is comparable to the change in the energy per unit charge of the normal ion flow across the shock according to estimates of varying sophistication for quasi-perpendicular shock geometry [Woods, 1969; Morse, 1973; Sanderson, 1976] (brackets denote change across the shock layer). Quasi-parallel shocks are less well understood. However, if the ions are principally decelerated by $[\phi]$, then it would be of comparable magnitude. At the earth's bow shock the net change in potential required in the frame where the plasma flows into the shock along the normal can be as high as 200–500 V. In general, the cross-shock potential change is frame dependent, being part of the four-dimensional vector potential [Jackson, 1962].

While there is general agreement that this cross-shock potential exists, relatively little attention has been paid to the frame dependence of the jump, $[\phi]$. This situation has led to some inaccuracy in the interpretation of both ion data [Greenstadt et al., 1980; Schwartz et al., 1983] and electron data [Feldman et al., 1982, 1983], where specific estimates made of the jump in one frame were implicitly or explicitly used in some other frame. The two frames most commonly used for

theoretical study of collisionless shocks are the normal incidence frame (NIF) (variables in this frame are denoted hereinafter by superscript N) and the de Hoffman–Teller frame (HTF) (variables in this frame are denoted hereinafter by superscript HT) [de Hoffman and Teller, 1950]. In the NIF the unshocked plasma velocity is collinear with the shock normal. In the HTF the asymptotic flow velocity and magnetic field are collinear on both sides of the shock layer. In this paper we focus on the behavior of electrons interacting with the cross-shock potential with three primary purposes: (1) to establish how electrons manage not to gain the potential energy lost by the ions; (2) to show that the frame dependence of this cross-shock potential reconciles the energy change determined in the HTF with that determined by an observer in the NIF; and (3) to establish the reversible, guiding center energy change expected for an electron fluid interacting with a steady state shock layer. We also address in some detail the corresponding implications for the ions of this frame dependence of the electrostatic potential which are especially important for ion reflection at the bow shock.

Since the observed change of the total electron energy in almost any frame is less than 50 eV [Montgomery et al., 1970; Scudder et al., 1973], electrons clearly do not gain the NIF potential energy lost by the ions. At the same time, at least for quasi-perpendicular shocks, the ions in the NIF are observed to be substantially slowed by an electrostatic field [Formisano, 1982; Greenstadt et al., 1980; Ogilvie et al., 1982]. Before observational data can be used to study the role of resistivities through the shock layer, the guiding center expectation of reversible behavior for an electron fluid needs to be determined. These results are explored by J. D. Scudder et al. (unpublished manuscript, 1984). In order to use data obtained in

Copyright 1984 by the American Geophysical Union.

Paper number 4A0566.
0148-0227/84/004A-0566\$05.00

the spacecraft frame of reference to address objective 3 a precise knowledge and understanding of the transformation of the cross-shock potential is required. These principles are clarified by reconciling the NIF and HTF descriptions of the electron's reversible energy change in section 2.

Two particular aspects of observed collisionless shock waves are crucial to the understanding of the reversible electron energy gain across shock waves.

1. The scale length R of the laminar fields is intermediate between the thermal electron gyroradius ρ_e and the incident (subscript 1) proton's streaming gyroradius in the NIF, $\rho_{i1} = V_{i1}^N / \Omega_{i1}$, where V_{i1}^N is the incident NIF ion bulk velocity and Ω_{i1} is the upstream ion gyrofrequency; this scaling has been well documented observationally [Russell and Greenstadt, 1979; Bame et al., 1979; Greenstadt et al., 1980; also Scudder et al., unpublished manuscript, 1984]. In this case the electrons are magnetized while the ions are not; while transiting the shock an electron's motion perpendicular to the shock normal is quite different from that of the ion; their ensemble average motion along the shock normal is of course the same, provided the shock layer is quasi-neutral and time stationary.

2. In addition to the electrostatic field \mathbf{E}_* along the shock normal, there is in general, except in the HTF, a motional electron field \mathbf{E}_M , due to the cross-field flow of the upstream plasma, which has components parallel to the shock surface that are conserved. The electric fields \mathbf{E}_* and \mathbf{E}_M can be derived from potentials ϕ_* and ϕ_M , respectively.

The related, but qualitatively different, picture of the interaction of electrons as viewed in the HTF is given in section 3, where the conserved components of \mathbf{E}_M^{HT} parallel to the shock surface vanish because $\mathbf{E}_M^{\text{HT}}(\pm\infty) \equiv 0$. Because electrons do not change their energy by drifting transverse to the shock normal in the HTF, they gain precisely the electrical potential energy lost by ions. However, an error can be made by assuming that $[\phi_*^{\text{HT}}]$ is identical to $[\phi_*^N]$, which can be conveniently estimated. In fact, $[\phi_*^{\text{HT}}]$ will be shown to be exactly small enough so that the electron energy gains in the HTF and NIF are consistent. The transformation properties of $[\phi_*]$ have important implications for discussions of ion and electron reflection, which for convenience are often discussed in the HTF, and require important modifications to the arguments of Schwartz et al. [1983] and Thomsen et al. [1983]. The requirement that the energy gain transform properly leads to the important conclusion that the spatial average of the magnetic field \mathbf{B} through the shock layer cannot lie in the coplanarity plane. This result is valid for arbitrary electron pressure and anisotropy and is a generalization of the isotropic pressure result [Tidman and Krall, 1971].

2. ELECTRON ENERGY GAIN IN THE NORMAL INCIDENCE FRAME

We adopt in this section the NIF for a detailed calculation of the reversible energy change expected across a time stationary shock. The results for an arbitrary frame such as the HTF are obtained, as below, by a Galilean/special relativistic transformation.

The NIF is defined such that the upstream plasma velocity is along the shock normal \hat{n} . As shown in Plate 1a, the x axis of the NIF is along \hat{n} , which points in the direction of increasing entropy. The upstream magnetic field \mathbf{B}_1 is in the x - z plane, which is often called the coplanarity plane as it is the common plane of both upstream and downstream flow velocity and magnetic field. The y axis is defined to complete a

right-handed coordinate system; it is antiparallel to the spatially averaged cross-field current density \mathbf{J} of a fast mode shock.

For the purposes of this paper, we make the following assumptions regarding the shock structure:

1. The shock structure is assumed to be time independent in the NIF or any other frame, such as the HTF, in which the shock is at rest. We thus neglect, for the present, the effects of time dependent phenomena, such as wave turbulence.

2. The shock layer is assumed to be one dimensional with spatial dependence in the force fields \mathbf{E} and \mathbf{B} only along the shock normal. This is quite reasonable on a macroscopic level. For the quasi-perpendicular shock the thin layer of the shock transition, which is $O(\rho_{i1})$, is much smaller than the radius of curvature ($\sim 15 R_E$) of the earth's bow shock. For the quasi-parallel shock the principal plasma transition (where $\mathbf{E}_* \neq 0$) appears also to occur on a scale small in relation to the radius of curvature [Scudder et al., 1984]. On the microscopic scale ($\sim c/\omega_{pe}$) there is certainly two- or three-dimensional structure due to the wave turbulence responsible for anomalous resistivity and heating in the shock which we neglect [Forsslund et al., 1984].

3. We assume that the scale length R of the magnetic and electric forces is intermediate between the electron gyroradius and the proton gyroradius.

The above assumptions allow a determination of the energy gain due to the macroscopic fields in the layer, which is a necessary first step in obtaining an observational determination of the anomalous heating or acceleration present.

2.1. Electron Potential Topology in NIF

The orientation of the electric field \mathbf{E}^N in the NIF is also indicated in Plate 1a. The electrostatic and motional components of \mathbf{E}^N have also been illustrated in Plate 1a, denoted \mathbf{E}_*^N and \mathbf{E}_M^N , respectively. The motional electric field is given by

$$\mathbf{E}_M^N = -\frac{1}{c} \mathbf{V}_{e1}^N \times \mathbf{B}_1 \quad (1)$$

where $\mathbf{V}_{e1}^N = \mathbf{V}_{sw}^N$ is the upstream electron fluid velocity in the NIF and \mathbf{B}_1 the asymptotic upstream magnetic field. Both \mathbf{V}_{e1} and \mathbf{B}_1 reside in the coplanarity plane also indicated in Plate 1a. The motional electric field is perpendicular to the coplanarity plane and given in the NIF by

$$\mathbf{E}_M^N = \frac{1}{c} |\mathbf{V}_{e1}^N| |\mathbf{B}_1| \sin \theta_{Bn} \hat{y} \quad (2)$$

where

$$\theta_{Bn} = \cos^{-1} (\mathbf{B}_1 \cdot \hat{n} / |\mathbf{B}_1|)$$

At this level of approximation the steady state assumption ($\nabla \times \mathbf{E} = 0$) implies that \mathbf{E}_M^N is conserved. Within the shock layer there exists a charge separation electric field \mathbf{E}_*^N which vanishes outside the layer and is orthogonal to the shock plane.

The electrical potential difference between two arbitrary points A and B connected in alphabetical order by the directed path denoted by C has contributions from both motional and electrostatic fields, namely,

$$[\phi^N]_C \equiv \phi_B^N - \phi_A^N = - \int_C \mathbf{E}^N \cdot d\mathbf{s}$$

In the normal incidence frame the potential difference with $A = (-\infty, y_0)$ and $B = (x, y)$ is given by

$$\begin{aligned}
& \phi^N(-\infty, y_0) - \phi^N(x, y) \\
&= (y - y_0) \frac{V_1 B_1}{c} \sin \theta_{Bn} + \int_{-\infty}^{+\infty} E_*^N(x) dx \\
&\equiv \phi_M^N(-\infty, y_0) - \phi_M^N(x, y) + \phi_*^N(-\infty, y_0) - \phi_*^N(x, y)
\end{aligned} \quad (3)$$

which defines the motional and electrostatic potentials for \mathbf{E}_M^N and \mathbf{E}_*^N , respectively. Thus although the forces \mathbf{E} and \mathbf{B} only vary along x , the potential field ϕ^N as explicitly determined above must depend on the y coordinate as well.

An illustrative model of the total electrical potential $\phi^N(x, y)$ is displayed in Plate 1b where ϕ_*^N has been chosen to be a monotonic function of x , namely,

$$\phi_*^N(x) = \frac{1}{2} [\phi_*^N] \{1 + \tanh(ax)\} \quad (4)$$

where $[\phi_*^N]$ is the change of the electrostatic potential when the path C is aligned with the normal. (The ensuing arguments apply, however, to any smoothly varying $\phi_*^N(x)$ including the nonmonotonic profiles found in the numerical simulations of supercritical quasi-perpendicular shocks discussed by Leroy et al. [1981, 1982]).

The potential topology shown in Plate 1b illustrates isocontours $\phi^N(x, y)$ in a plane orthogonal to the coplanarity plane through the shock layer. The blue curves are the isocontours of the electrical potential $\phi^N(x, y)$ as determined from equations (3) and (4). The red vertical lines are the isocontours of $\phi_*^N(x, y)$. The negative gradients of ϕ_*^N , not ϕ^N , determine the electrostatic cross-shock electric field. The displacement of a particle with respect to the blue isocontours of $\phi^N(x, y)$ determines the energy change that results from interacting with the smooth forces at the shock layer.

The topology of the blue isocontours of ϕ^N is generically correct for any θ_{Bn} shock orientation, save the ideally singular $\theta_{Bn} = 0$ parallel shock, since the existence of equipotential contours of ϕ^N crossing the shock layer only depends on the existence of $\mathbf{E}_M^N \neq 0$.

Since $\rho_e < R < \rho_i$, the paths of initially coincident electrons and ions, C_e and C_i respectively, are different. The magnitudes of the changes in their energies

$$\begin{aligned}
| -e[\phi^N]_{C_e} | &\equiv \lim_{x \rightarrow \infty} e \{ \phi^N(x, y_e', z_e') - \phi^N(-x, y_e, z_e) \} \\
| e[\phi^N]_{C_i} | &\equiv \lim_{x \rightarrow \infty} e \{ \phi^N(x, y_i', z_i') - \phi^N(-x, y_e, z_e) \}
\end{aligned}$$

will not be equal but will be proportional to the difference in electrical potential between the asymptotic downstream trajectories of an initially collocated electron ion pair

$$[\phi^N]_e - [\phi^N]_i = \lim_{x \rightarrow \infty} \{ \phi^N(x, y_e, z_e) - \phi^N(x, y_i, z_i) \} \neq 0$$

2.2. Electron Energy Gain

The net energy change of an individual electron in traversing the shock layer in the NIF is given by

$$\Delta \varepsilon^N = \int_c \frac{d}{dt} \left(\frac{1}{2} m_e |v_e^N|^2 \right) dt = -e \int_c \mathbf{v}_e^N \cdot \mathbf{E}^N dt \quad (5)$$

where the path integrals \int_c are along the electron trajectory through the shock. The elemental positive charge is denoted by e . Since $\mathbf{E}^N \equiv \mathbf{E}_M^N + \mathbf{E}_*^N$, we expand the right-hand side of (5) as

$$\Delta \varepsilon^N = -e \int_c \mathbf{v}_e^N \cdot (\mathbf{E}_*^N + \mathbf{E}_M^N) dt \quad (6a)$$

$$\Delta \varepsilon^N = e \int_c \mathbf{v}_G \cdot \hat{n} \frac{d}{dx} \phi_*^N dt - e \int_c \mathbf{v}_G^N \cdot \mathbf{E}_M^N dt \quad (6b)$$

$$\Delta \varepsilon^N \equiv e[\phi_*^N] - e \int_c \mathbf{v}_G^N \cdot \mathbf{E}_M^N dt \quad (6c)$$

The first term in (6c) is the energy a hypothetically unmagnetized electron would gain in traversing the electrostatic shock potential $[\phi_*^N]$ (crossing red lines in Plate 1b). The second term represents the guiding center drift work against the motional electric field \mathbf{E}_M^N .

Within our assumption of guiding center ordering for electron dynamics, \mathbf{E} is approximately constant over an electron gyroradius ρ_e , and any change to the right-hand side of (5) depends on the guiding center velocity \mathbf{v}_G . In a steady state system, \mathbf{v}_G is given [Northrop, 1963] in NIF by

$$\begin{aligned}
\mathbf{v}_G^N &= v_{\parallel e}^N \hat{b} + \mathbf{U}_E^N \\
&- c \frac{\hat{b}}{B} \times \left\{ \mu \nabla B + \frac{m}{e} v_{\parallel}^N \left(v_{\parallel}^N \frac{\partial}{\partial s} + \mathbf{U}_E^N \cdot \nabla \right) \hat{b} \right. \\
&\left. + \frac{m}{e} \left(v_{\parallel} \frac{\partial}{\partial s} + \mathbf{U}_E^N \cdot \nabla \right) \mathbf{U}_E^N \right\}
\end{aligned} \quad (7)$$

In the preceding equation, $\mu \equiv m w_{\perp}^2 / 2eB$ is the electron magnetic moment, w_{\perp} is the magnitude of the gyration velocity around the guiding center, $\mathbf{U}_E^N = c \mathbf{E}^N \times \mathbf{B} / B^2$ is the electric field drift, and $\partial / \partial s = \hat{b} \cdot \nabla$ is the derivative along \hat{b} . The first two terms, the parallel motion of the guiding center $v_{\parallel e}$ and the electric drift \mathbf{U}_E^N , are independent of the gradients of \mathbf{B} and are zero order in an expansion in gyroradius over the scale length of the electrostatic field. The remaining terms are of higher order and will be referred to as finite Larmor radii (FLR) corrections.

2.2.1. Infinitesimal Larmor radius limit. The zero-order terms, $v_{\parallel} \hat{b}$ and \mathbf{U}_E , are potentially the largest contributions to \mathbf{v}_G^N . In fact, for thermal electrons at shocks in the solar-terrestrial environment these terms dominate \mathbf{v}_G^N . These motions can then potentially result in much larger energy gains than are possible from the grad B and curvature drifts. We feel it is instructive to examine in some detail the effects of the zero-order motions alone, i.e., consider the infinitesimal Larmor radius (ILR) limit.

Using the ILR expansion for \mathbf{v}_G in the second term of (6c), we can explicitly exhibit the work done by the guiding center drifts against the motional electric field:

$$\Delta \varepsilon_e^N = e[\phi_*^N] - e \int_c (v_{\parallel}^N \hat{b} + \mathbf{U}_E^N) \cdot \mathbf{E}_M^N dt \quad (8a)$$

$$\Delta \varepsilon_e^N = -e \int_c \mathbf{v}_G^N \cdot \mathbf{E}_*^N dt - e \int_c \mathbf{U}_E^N \cdot (\mathbf{E}^N - \mathbf{E}_*^N) dt \quad (8b)$$

$$\Delta \varepsilon_e^N = -e \int_c \mathbf{v}_G^N \cdot \mathbf{E}_*^N dt + 0 + e \int_c \mathbf{U}_E^N \cdot \mathbf{E}_*^N dt \quad (8c)$$

$$\Delta \varepsilon_e^N = -e \int_c v_{\parallel}^N E_{* \parallel}^N dt \quad (8d)$$

The work done in drifting along \mathbf{E}_M^N significantly reduces the unmagnetized electron electrostatic energy gain $e[\phi_*^N]$ with the net result that only the component of \mathbf{E}_*^N along \hat{b} contributes to the energy change. This conclusion is the corollary of the fact that \mathbf{U}_E drifts can do no work. This calculation does, however, illustrate graphically the competing effects involved. An electron does gain energy equivalent to that lost by an ion

in traversing the shock potential. However, since the magnetized electron must drift against \mathbf{E}_M , much of this energy is lost. For a perpendicular shock, the work done against \mathbf{E}_M equals the electrostatic gain. For the opposite limit, an ideal time stationary parallel shock, $\mathbf{E}_M^N = 0$, and an electron gains the entire electrostatic potential.

2.2.2. *Energy gain for finite Larmor radius (FLR).* The first-order drifts in (7) result in energy changes due to the inhomogeneity of the shock magnetic field. These energy changes are roughly proportional to μ and are limited generally to approximately $4KT_e$, which is much less than the electrostatic potential jump in the normal incidence frame. However, since $e\Delta\phi_*^N$ cannot be fully converted into electron energy, these effects are generally significant for oblique shocks and dominate for quasi-perpendicular shocks.

If we consider the differential form of (5) and use (7) for \mathbf{v}_G^N , we obtain [Northrop, 1963]

$$\begin{aligned} \frac{d}{dt} \epsilon^N = & -e \left\{ v_{\parallel}^N E_{* \parallel}^N \right. \\ & - \mathbf{E}^N \cdot \left\{ \frac{c\hat{b}}{B} \times \left(\mu \nabla B + \frac{mv_{\parallel}^N}{e} \left(v_{\parallel}^N \frac{\partial}{\partial s} + \mathbf{U}_E^N \cdot \nabla \right) \hat{b} \right. \right. \\ & \left. \left. + \frac{m}{e} \left(v_{\parallel}^N \frac{\partial}{\partial s} + \mathbf{U}_E^N \cdot \nabla \right) \mathbf{U}_E^N \right\} \right\} \end{aligned} \quad (9a)$$

$$\begin{aligned} \frac{d}{dt} \epsilon^N = & -ev_{\parallel}^N E_{* \parallel}^N + e\mu(\mathbf{U}_E^N \cdot \nabla)B + mv_{\parallel}^N \mathbf{U}_E^N \cdot \frac{d}{dt} \hat{b} \\ & + \frac{d}{dt} \left\{ \frac{1}{2} m(U_E^N)^2 \right\} \end{aligned} \quad (9b)$$

where we have used

$$\frac{d}{dt} \simeq \frac{\partial}{\partial s} + \mathbf{U}_E^N \cdot \nabla$$

The first term on the right-hand side is the ILR electrostatic energy gain. The second and third terms are the betatron and curvature drift terms, and the last is the guiding center acceleration term.

The additional terms in (9) represent the work done by the grad B and curvature drifts against \mathbf{E}^N . The betatron term is proportional to changes in the magnitude of \mathbf{B} and implies that μ is conserved. The curvature term is proportional to changes in the direction of \mathbf{B} . The betatron and the curvature effects generally have opposite signs in magnetosonic shock waves. Since these corrections are proportional to the change in \mathbf{B} , the fast and slow mode shocks differ in which pitch angles benefit from the drift work: in the fast mode shocks the betatron effect increases the perpendicular energy, while the curvature drifts extract kinetic energy from the parallel electron motions. For the slow mode shock the betatron effect decreases the perpendicular kinetic energy, and curvature drifts increase the parallel kinetic energy. For either shock the energy gain from the electrostatic field is always nonnegative when the electron goes from the undisturbed to the shocked side of the layer. These results are summarized in Table 1.

3. THE DE HOFFMAN-TELLER FRAME

The calculations in the normal incidence frame illustrate the interaction of the electron motions along \mathbf{E}_*^N and \mathbf{E}_M^N in traversing the shock. Of course, the energy gain can be similarly calculated in any inertial reference frame in which the shock is at rest. For a one-dimensional planar shock, there are

TABLE 1. Net Energy Gain

Electrostatic	Betatron	Curvature	Shock Type
+	+	-	fast mode
+	-	+	slow mode

an infinite set of such frames with different relative motions perpendicular to \hat{n} . Since \mathbf{E} and \mathbf{B} are frame dependent, the kinematics of the electron behavior in crossing the shock vary. However, the results for any frame are related to those for the NIF via a Galilean (or special relativistic) transformation and must be consistent.

The de Hoffman-Teller frame (HTF) is a particularly useful shock rest frame in which \mathbf{E}_M vanishes. The electron kinematics in the HTF differs radically from that described above. In this frame the electron drifts perpendicular to \hat{n} do no work to offset the energy gained from the electrostatic field; an electron gains the full electrostatic potential energy jump across the shock. We show here that when the transformation properties of \mathbf{E}_* (and thus ϕ_*) are considered, the results in either the HTF and NIF properly agree.

The HTF moves in relation to the NIF with a velocity

$$\mathbf{V}_{HT}^N \equiv V_{HT}^N \hat{z} = -V_1^N \tan \theta_{Bn} \hat{z} \quad (10)$$

For $\theta_{Bn} < 88.5^\circ$ and $V_1^N \sim 300$ km/s, V_{HT}^N is nonrelativistic. The electric field in this frame is given by

$$\mathbf{E}^{HT} = (\mathbf{E}^N + \frac{1}{c} \mathbf{V}_{HT}^N \times \mathbf{B}^N) \quad (11)$$

By definition the components of \mathbf{E}^{HT} perpendicular to \hat{n} are zero throughout the shock. Therefore the electron energy gain in the HTF is

$$\begin{aligned} \frac{d}{dt} \epsilon^{HT} = & -e(\mathbf{v}^{HT} \cdot \mathbf{E}^{HT}) = -ev_x^{HT} E_*^{HT} \\ = & -ev_x^N E_*^{HT} \end{aligned} \quad (12)$$

where we have used the fact that v_x is the same in both frames to within relativistic corrections.

While E_*^{HT} equals E_*^N upstream and downstream of the shock (they both vanish), E_*^{HT} is related in general to E_*^N by

$$E_*^{HT} = (E_*^N - \frac{1}{c} V_{HT}^N B_y^N) \quad (13)$$

where explicit use has been made of the fact that \mathbf{V}_{HT}^N has only a z component. We can write B_y^N in terms of \mathbf{v}_e^N by considering the z component of an electron's equation of motion in the NIF,

$$B_y^N = \frac{v_{ey}^N}{v_{ex}^N} B_x - \frac{mc}{ev_{ex}^N} \frac{d}{dt} v_{ez}^N \quad (14)$$

Using these results, we can write $(\mathbf{v} \cdot \mathbf{E})^{HT}$ of (12) in terms of \mathbf{v}_*^N and \mathbf{E}^N :

$$\begin{aligned} (\mathbf{v} \cdot \mathbf{E})^{HT} = & \left(v_x^N E_*^N + v_y^N E_y^N + \frac{m}{e} \mathbf{V}_{HT}^N \cdot \frac{d}{dt} \mathbf{v}^N \right) \\ = & (\mathbf{v} \cdot \mathbf{E})^N + \frac{1}{e} \frac{d}{dt} (m_e \mathbf{V}_{HT}^N \cdot \mathbf{v}^N) \end{aligned} \quad (15a)$$

i.e.,

$$\frac{1}{2} \frac{d}{dt} m_e |\mathbf{v}^{HT}|^2 = \frac{1}{2} \frac{d}{dt} m_e |\mathbf{v}^N - \mathbf{V}_{HT}^N|^2 \quad (15b)$$

where use has been made again of the fact that v_x^N is equal to its counterpart in the HTF except for relativistic frame changes. Because of the transformation properties of \mathbf{E}_* , the energy gain for electrons in the HTF is shown to be essentially the same as in the NIF. The second term is due to the change of the electron velocity along the relative frame velocity. This term is normally small, being proportional to the electron mass.

In retrospect, (15b) is a basic tenet of Galilean kinematics, and the arguments used to reach it, equations (13)–(15a), can be inverted to prove that the spatial average of \mathbf{B}_y^N need be nonzero. Considering the perpendicular limit ($B_x \rightarrow 0$) of (13) by inserting $B_y = 0$ gives the misleading idea that $E_*^{\text{HT}} = E_*^N$. Because V_{HT} is $O(1/B_x)$, this is not the correct evaluation of the limit, and the behavior of quasi-perpendicular shock electrostatic fields in the two frames requires that the limit be carefully considered as in (15).

The difference between $[\phi_*^N]$ and $[\phi_*^{\text{HT}}]$ implies that the particle kinematics in the two frames will have different emphasis. In particular, the electrostatic forces are usually more important than the magnetic forces in the NIF and vice versa in the HTF.

To estimate the size of $[\phi_*^{\text{HT}}]$ relative to $[\phi_*^N]$, we note that $\mathbf{E} \cdot \mathbf{B}$ is a (relativistic) frame independent scalar [e.g., Jackson, 1962]. In the HTF, $\mathbf{E}^{\text{HT}} = \mathbf{E}_*^{\text{HT}}$, and it is along the shock normal. Therefore

$$\mathbf{E}^{\text{HT}} \equiv \frac{E_{\parallel}^{\text{HT}}}{(\hat{n} \cdot \hat{b})} \hat{n} = \frac{E_{\parallel}^N}{(\hat{n} \cdot \hat{b})} \hat{n}$$

From the generalized Ohm's law [Rossi and Olbert, 1970],

$$E_{\parallel}^N \approx \frac{-\hat{b} \cdot \nabla \cdot \mathbf{P}_e}{en_e}$$

to within electron inertial corrections, where \mathbf{P}_e is the electron pressure tensor. Therefore if \mathbf{P}_e is gyrotropic, then

$$E_*^{\text{HT}} \sim -\frac{1}{en_e} \left\{ \frac{d}{dx} P_{e\parallel} - (P_{e\parallel} - P_{e\perp}) \frac{d}{dx} \ln B \right\} \quad (16)$$

where $\mathbf{P}_e \equiv P_{e\parallel} \hat{b}\hat{b} + P_{e\perp}(1 - \hat{b}\hat{b})$. We can integrate this equation to get $[\phi_*^{\text{HT}}]$ if we ignore anisotropic effects and assume $P_e \propto n_e^\gamma$ with the result

$$[e\phi_*^{\text{HT}}] \approx \frac{\gamma}{(\gamma - 1)} [kT_e] \quad (17)$$

Observationally, γ appears to be $\frac{5}{3} \sim 2$ [Feldman et al., 1982], so that $e[\phi_*^{\text{HT}}]$ is observationally [Montgomery et al., 1970; Scudder et al., 1973; Formisano, 1982] much less than

$$e[\phi_*^N] \approx -[\frac{1}{2}m_i(V_i^N \cdot \hat{n})^2] \quad (18)$$

Comparison of the magnitudes of (17) and (18) together with (10) and (13) implies that the spatial average of B_y/B_{x1} must, in fact, be positive. The strong frame dependence of $[\phi_*]$ illustrated here has not always been acknowledged in the literature [Greenstadt et al., 1980; Feldman et al., 1982, 1983; Schwartz et al., 1983; Thomsen et al., 1983].

Clearly, $[\phi_*^{\text{HT}}]$ is insufficient to lead to a significant deceleration of the ions; the ion deceleration in the HTF is accomplished primarily by magnetic forces via the retarding force $-(1/c)V^{\text{HT}}B_y$. The internal magnetic structure of the shock, i.e., $B_y(x)$, is of primary importance to the ion dynamics in the HTF; while present in the NIF, the Lorentz terms are less important. This strongly implies that internal shock structure

cannot be ignored in the HTF, i.e., the common assumption of an infinitesimally thin shock layer is not valid.

4. ADIABATIC CONSERVATION EQUATIONS FOR AN ELECTRON FLUID WHEN $df/dt = 0$

A major motivation for this paper has been to predict the adiabatic changes of the electron energy at shock waves to allow comparisons with observed values at interplanetary and planetary bow shocks, and to determine any nonadiabatic heating present. Nonadiabatic heating via short-wavelength wave turbulence is a common feature of collisionless shock theory [e.g., Tidman and Krall, 1971; Wu et al., 1984]. While a substantial body of observational wave data for the earth's bow shock and other shocks exists and much theoretical effort and attention has been given to the linear, and to a lesser extent, nonlinear behavior of several interesting wave modes, it has proven difficult to identify the wave modes and sources of the observed waves, and more difficult to predict electron heating levels. Observational determinations of the nonadiabatic electron heating would be very useful in identifying the important wave processes, if any.

In order to be useful in this context, the individual electron result in the NIF in (9) must be averaged over the electron distribution function f_e to obtain an expression for the electron fluid parameters commonly available from spacecraft observations. If we denote this average by angle brackets, we find, considering the right-hand side first,

$$\begin{aligned} \left\langle \frac{d}{dt} \varepsilon^N \right\rangle &= -neV_{\parallel}^N E_{*\parallel}^N + n \frac{kT_{\perp}}{B} \mathbf{V}_{\perp}^N \cdot \nabla B \\ &+ n\mathbf{V}_{\perp}^N \cdot \left\{ kT_{\parallel} + m(V_{\parallel}^N)^2 \right\} \frac{\partial \hat{b}}{\partial s} \\ &+ mV_{\parallel}^N (\mathbf{V}_{\perp} \cdot \nabla) \hat{b} \left. \right\} + \nabla \cdot \left(\frac{n}{2} m |\mathbf{V}_{\perp}^N|^2 \mathbf{V}^N \right) \quad (19a) \end{aligned}$$

For a steady state plasma the left-hand side of the above equation is just the divergence of the electron energy flux:

$$\left\langle \frac{d}{dt} \varepsilon^N \right\rangle = \nabla \cdot \{ \mathbf{Q}_e + \text{Tr}(\mathbf{P}_e) \mathbf{V}^N + (\mathbf{V}^N \cdot \mathbf{P}_e) + \frac{1}{2} nm |\mathbf{V}^N|^2 \mathbf{V}^N \} \quad (19b)$$

In the above equations, $\mathbf{V} = (V_{\parallel} \hat{b} + \mathbf{V}_{\perp})$ is the electron bulk velocity, \mathbf{P} is the pressure tensor, and \mathbf{Q}_e is the electron heat flux in the electron bulk frame.

Equations (19a) and (19b) are valid only in the NIF, and observed plasma and field properties must be transformed to this frame before being used.

5. DISCUSSION AND SUMMARY

In this paper we have studied the adiabatic energy gain of electrons in the stationary electric and magnetic field structure of collisionless shock waves. We have resolved the apparent contradiction of the seemingly different energy gains of electrons in the NIF and HTF by showing that \mathbf{B} in the shock layer must have a positive (negative) spatially averaged component orthogonal to the coplanarity plane (except for $\theta_{\text{bn}} = 90^\circ$) when B_{x1} is positive (negative). This in turn implies that the cross-shock electrostatic potential jump along the normal is smaller in the HTF than in the NIF except for the exactly parallel shock. From the guiding center energy gain for individual electrons we have determined the electron fluid energy

NORMAL INCIDENCE FRAME (NIF)

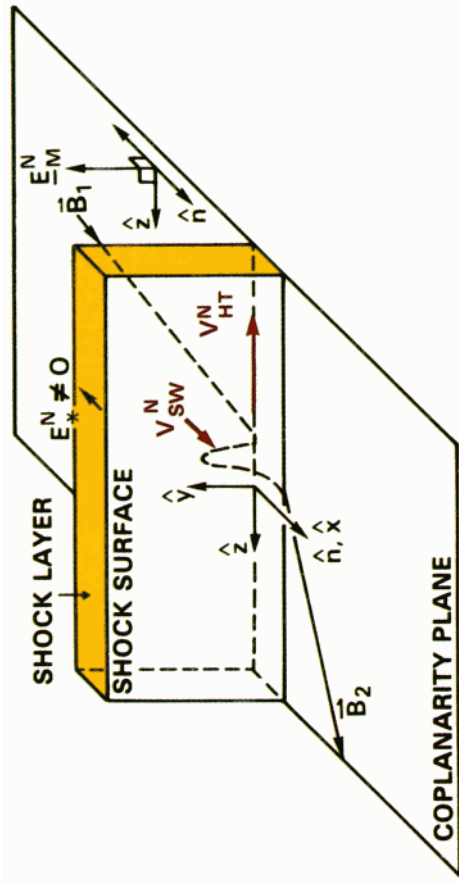


Plate 1a

(NIF)

ISOPOTENTIALS OF MODEL Q-PERP SHOCK LAYER

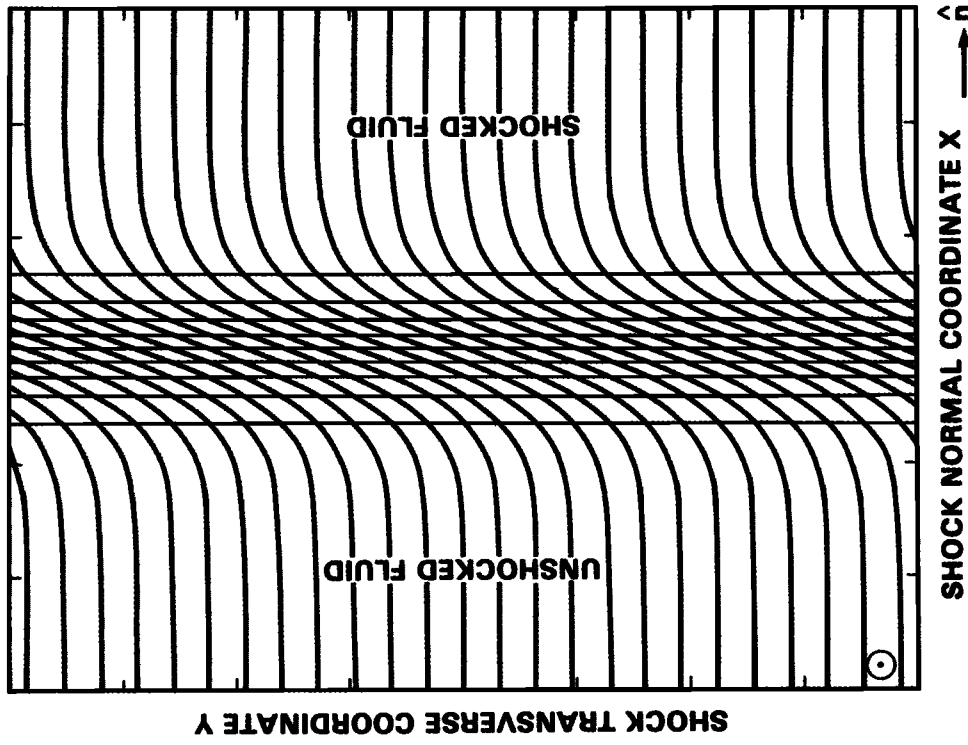


Plate 1b

Plate 1. (a) Geometrical relationships of the electric and magnetic fields in the normal incidence frame (NIF) in which the upstream plasma velocity V_1^N is normal to the shock plane. Note that E^N has both a conserved component E_M^N , tangential to the plane of the shock, and a spatially varying component E_*^N , which is collinear with the shock normal and vanishes outside the layer. B_1 , V_1^N , B_2 , and V_2^N are in the coplanarity plane. However, B must in general have components out of the coplanarity plane within the shock layer. (b) Representative topology of the cross-shock electrical potential showing isocontours of ϕ^N (blue curves) and ϕ_*^N (red curves). Shock coordinates are used: y vertical and x horizontal as in Plate 1a.

NORMAL INCIDENCE FRAME (NIF)

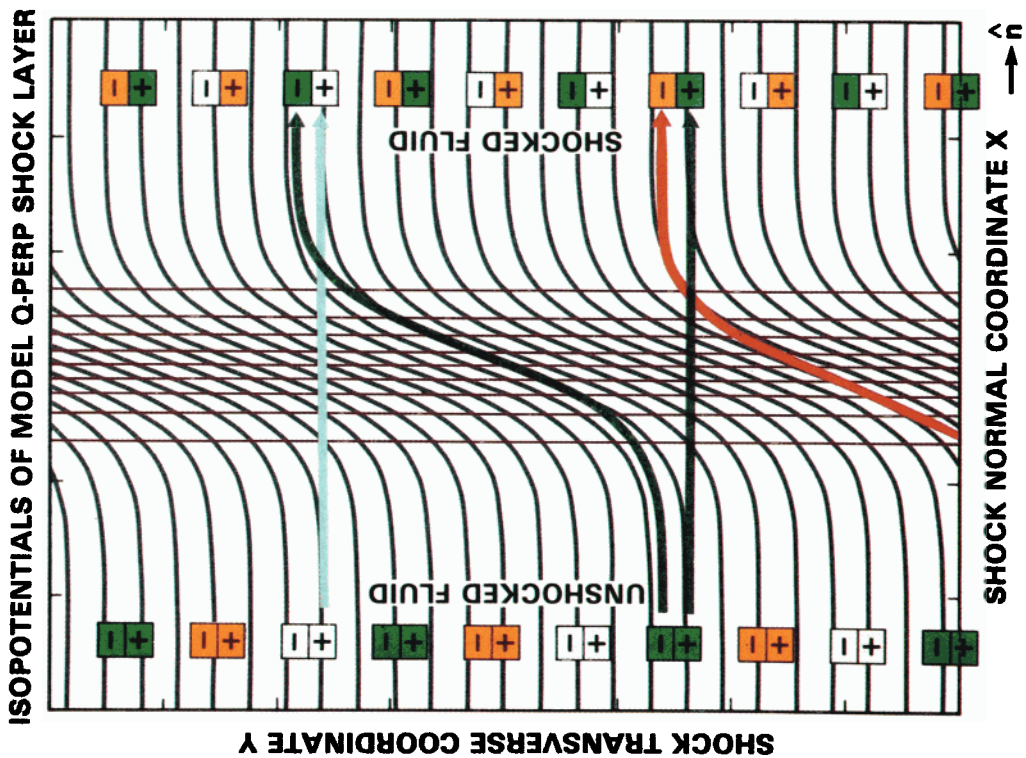


Plate 2a

Plate 2. (a) Plate 1b has been augmented to illustrate the different ion and electron paths through the shock layer in the NIF. The electron gyroradius has been assumed small and the ion gyroradius large in comparison to the scale of the layer. (b) Same format as Plate 2a for the de Hoffman-Teller frame, HTF. Note that electron and ion trajectories are the same, while potential topology is radically different. The same contour levels are assumed in Plates 2a and 2b. Here $[\phi_*^{HTF}]$ has been assumed to be $\sim \frac{1}{10} [\phi_*^N]$.

DEHOFFMAN - TELLER FRAME (HTF)

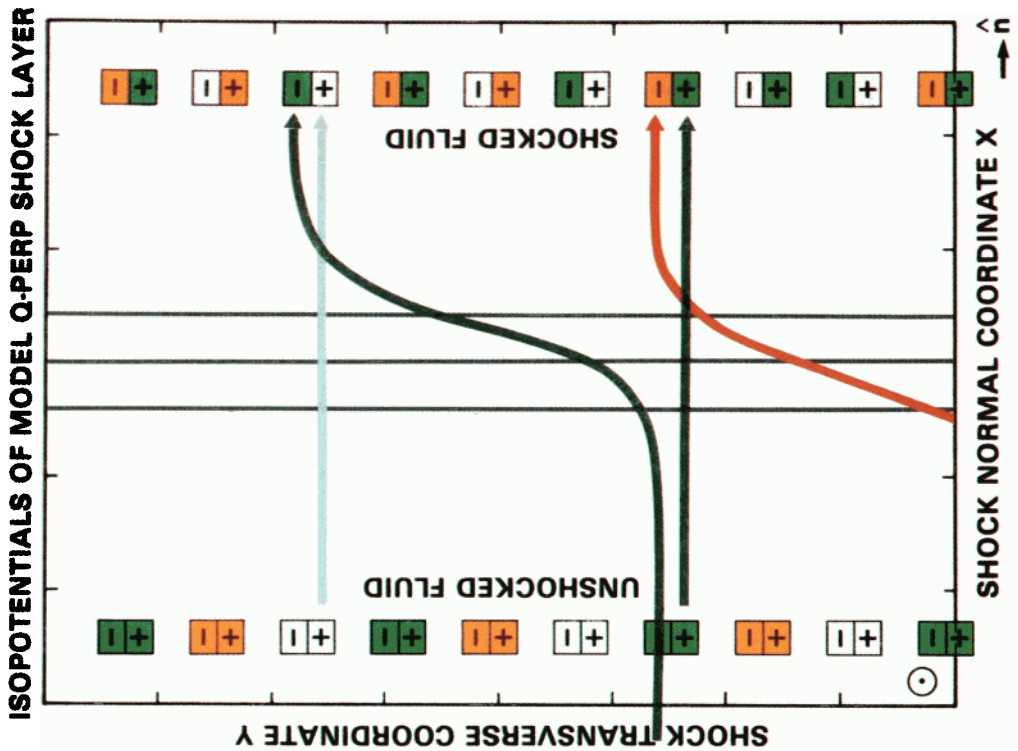


Plate 2b

conservation equation under the adiabatic assumption which is used by Scudder et al. (unpublished manuscript, 1984) to infer dissipation at a well-documented shock wave. Understanding the adiabatic electron energy gain is crucial to any observational attempt to study nonadiabatic heating mechanisms such as wave heating.

The key factor in the electron behavior is that the scale length of the shock gradients is intermediate between the electron and proton gyroradii. The ions are essentially unmagnetized; in the NIF they are primarily slowed by the shock electrostatic field with a magnitude $[q\phi_*^N] \sim [\frac{1}{2}m_i(\mathbf{V}_i^N \cdot \hat{n})^2]$ which is several hundred electron volts at the earth's bow shock. By contrast, the magnetized electrons change their energy in the shock layer as determined by their guiding center motion. The results of Northrop [1963] lead to the result (sections 2.2.1 and 2.2.2) that only the component of \mathbf{E}_*^N parallel to \hat{b} contributes to the net energy gain. For quasi-perpendicular and oblique shocks in the NIF the energy gain in the ILR limit for electrons is small; the observed energy gain of the electrons is controlled by the magnetic gradient drifts (FLR effects).

For quasi-parallel shocks these calculations suggest that the net reversible energy gain for electrons from the electrostatic field should be dominant and approach the change in the ion bulk energy if the cross-shock potential for $\theta_{bn} \approx 0$ does approach $[\frac{1}{2}M(\mathbf{V} \cdot \hat{n})^2]$. This is, in fact, contrary to observations [Scudder et al., 1984]. If, in fact, a potential large enough to decelerate the ions exists in quasi-parallel shocks, then one or more of the effects we neglected must act either to keep $\mathbf{E} \cdot \hat{b} \approx 0$ or to create sufficient electron-ion energy coupling to counteract the large electron energy gain that results otherwise. Additional observational and theoretical investigation is needed to determine the importance of the most probable effects: (1) time dependence, (2) two- or three-dimensional structure, or (3) wave turbulence.

The different behavior of transmitted electrons and ions in the NIF is summarized in Plate 2a for a perpendicular shock. This figure has the same format as Plate 1b. The incoming ion-electron pairs are shown to the left as similarly colored squares. The transmitted ions of each pair move directly across the shock layer, crossing isopotentials of the total electrical potential (blue curves), and losing energy to the electrostatic potential (red lines). The electrons drift in the y direction while progressing across the layer. In so doing they gain energy crossing isocontours of ϕ_*^N (red) and lose it by moving orthogonal to isocontours of the motional potential ϕ_M^N . The net energy gain is due to finite Larmor radius effects and is proportional to the gradient of \mathbf{B} . An equivalent viewpoint is that the magnetized electrons move nearly along the equipotentials of the total electric field (blue contours).

In the HTF the motional electric field vanishes, and the equipotentials of ϕ_M^{HT} and ϕ_*^{HT} are identical and both parallel to the shock surface (Plate 2b). In this frame the electron energy gain from the electrical potential including finite Larmor radius effects is precisely what a transmitted ion loses to this potential, as shown in Plate 2b. However, the potential jump along the normal in this frame $[\phi_*^{\text{HT}}]$ has been shown to be much smaller than $[\phi_*^N]$ in the approximate ratio

$$[\phi_*^{\text{HT}}]/[\phi_*^N] \sim -\left(\frac{\gamma}{\gamma-1}\right)[kT_e]/[\frac{1}{2}m_i(\mathbf{V}_i^N \cdot \hat{n})^2]$$

which is approximately $\frac{1}{10} - \frac{1}{3}$ at the earth's bow shock. In this way the electron energy gain in the HTF is reconciled to

that of the NIF observer. The numerical difference has been shown to be that expected for the Galilean transformation of energy (cf. equation (15)) and for electrons is small.

The required frame dependence of $[\phi_*]$ has important implications for the ion kinematics as well. In the HTF, $[\phi_*^{\text{HT}}]$ is too small to slow down the transmitted ions. In this frame the Lorentz force proportional to B_y dominates the normal motion of the ions. Since B_y is out of the coplanarity plane and can be nonzero only within the shock layer, careful consideration of internal shock structure is essential for the study of electron and ion dynamics in the HTF. In particular, the use of infinitesimally thin shock layers to study ion reflection processes is probably not valid.

The net reversible work done on electrons in either NIF or HTF is most nearly synonymous with the de Hoffman-Teller cross-shock potential jump $[e\phi_*^{\text{HT}}]$. Accordingly, features of the electron distribution function are sensitive to ϕ_*^{HT} , not ϕ_*^N as implied by Feldman et al. [1982, 1983]. Conversely, the work done by ions is most directly determined by $[e\phi_*^N]$. If for convenience the HTF is adopted for ion leakage arguments as is commonly done, then ϕ_*^{HT} must be consistently used, as opposed to the assumptions in the papers by Schwartz et al. [1983], Thomsen et al. [1983], and Schwartz and Burgess [1984]. Finally, the ion energy loss is strongly frame dependent. The ion energy change in the spacecraft frame need not be related to $[\phi_*^N]$ as was suggested by Greenstadt et al. [1980], since ϕ_*^N only changes the energy associated with normal components of the bulk flow of the ions in the shock frame.

Acknowledgments. We would like to acknowledge helpful discussions with M. Leroy. This work is partially supported by the NASA Solar Terrestrial Theory Program (grant NAGW-81)

The Editor thanks E. W. Greenstadt and R. P. Lin for their assistance in evaluating this paper.

REFERENCES

- Bame, S. J., J. R. Asbridge, J. T. Gosling, M. Halbig, G. Paschmann, N. Sckopke, and H. Rosenbauer, High temporal resolution observations of electron heating at the bow shock, *Space Sci. Rev.*, **23**, 75, 1979.
- de Hoffman, F., and E. Teller, Magneto-hydrodynamic shocks, *Phys. Rev.*, **80**, 692, 1950.
- Feldman, W. C., R. C. Anderson, J. R. Asbridge, S. J. Bame, J. T. Gosling, and R. D. Zwickl, Plasma electron signature of magnetic connection to the earth's bow shock: ISEE 3, *J. Geophys. Res.*, **87**, 632, 1982.
- Feldman, W. C., R. C. Anderson, S. J. Bame, S. P. Gary, J. T. Gosling, D. J. McComas, M. F. Thomsen, G. Paschmann, and M. M. Hoppe, Electron velocity distributions near the earth's bow shock, *J. Geophys. Res.*, **88**, 96, 1983.
- Formisano, V., Measurement of the potential drop across the earth's collisionless bow shock, *Geophys. Res. Lett.*, **9**, 1033, 1982.
- Forsslund, D. W., K. B. Quest, J. U. Brackbill, and K. Lee, Collisionless dissipation in quasi-perpendicular shocks, *J. Geophys. Res.*, **89**, 2142, 1984.
- Greenstadt, E. W., et al., A macroscopic profile of the typical quasi-perpendicular shock: ISEE 1 and 2, *J. Geophys. Res.*, **85**, 2124, 1980.
- Jackson, J. D., *Classical Electrodynamics*, John Wiley, New York, 1962.
- Leroy, M. M., C. C. Goodrich, D. Winske, C. S. Wu, and K. Papadopoulos, Simulation of a perpendicular bow shock, *Geophys. Res. Lett.*, **8**(12), 1269, 1981.
- Leroy, M., D. Winske, C. C. Goodrich, C. S. Wu, and K. Papadopoulos, The structure of perpendicular bow shocks, *J. Geophys. Res.*, **87**, 5081, 1982.
- Montgomery, M. D., J. R. Asbridge, and S. J. Bame, VELA 4 Plasma observations near the earth's bow shock, *J. Geophys. Res.*, **75**, 1217, 1970.

- Morse, D. L., Electrostatic potential rise across perpendicular shocks, *Plasma Phys.*, *15*, 1262, 1973.
- Northrop, T. G., *The Adiabatic Motion of Charged Particles*, Wiley Interscience, New York, 1963.
- Ogilvie, K. W., M. A. Coplan, and R. D. Zwickl, Helium, hydrogen, and oxygen velocities observed on ISEE 3, *J. Geophys. Res.*, *87*, 7363, 1982.
- Rossi, B., and S. Olbert, *Introduction to the Physics of Space*, McGraw-Hill, New York, 1970.
- Russell, C. T., and E. W. Greenstadt, Initial ISEE magnetometer results: Shock observations, *Space Sci. Rev.*, *23*, 3, 1979.
- Sanderson, J. J., Jump conditions across a collisionless, perpendicular shock, *J. Phys.*, *9*, 2327, 1976.
- Schwartz, S. J., and D. Burgess, On the theoretical/observational comparison of field-aligned ion beams in the earth's foreshock, *J. Geophys. Res.*, *89*, 2381, 1984.
- Schwartz, S. J., M. F. Thomsen, and J. T. Gosling, Ions upstream of the earth's bow shock: A theoretical comparison of alternative source populations, *J. Geophys. Res.*, *88*, 2039, 1983.
- Scudder, J. D., K. W. Ogilvie, and D. Lind, Electron observations in the solar wind and magnetosheath, *J. Geophys. Res.*, *78*, 28, 1973.
- Scudder, J. D., L. F. Burlaga, and E. W. Greenstadt, Scale lengths in quasi-parallel shocks, *J. Geophys. Res.*, in press, 1984.
- Thomsen, M. F., S. J. Schwartz, and J. T. Gosling, Observational evidence on the origin of ions upstream of the earth's bow shock, *J. Geophys. Res.*, *88*, 7483, 1983.
- Tidman, D. A., and N. A. Krall, *Shock Waves in Collisionless Plasmas*, Wiley Interscience, New York, 1971.
- Woods, L. C., Jump conditions for a two-fluid magneto-plasma, *Plasma Phys.*, *11*, 967, 1969.
- Wu, C. S., et al., Microinstabilities associated with a high Mach number perpendicular bow shock, *Space Sci. Rev.*, *37*, 63, 1984.
-
- C. C. Goodrich, Astronomy Program, University of Maryland, College Park, MD 20742.
J. D. Scudder, Mail Code 692, NASA Goddard Space Flight Center, Greenbelt, MD 20771.

(Received May 24, 1982;
revised April 9, 1984;
accepted April 11, 1984.)